

RESEARCH

Open Access



# Head-to-head comparison of plasma and PET imaging ATN markers in subjects with cognitive complaints

Jiaying Lu<sup>1,2†</sup>, Xiaoxi Ma<sup>2,3†</sup>, Huiwei Zhang<sup>1,2</sup>, Zhenxu Xiao<sup>2,3</sup>, Ming Li<sup>1</sup>, Jie Wu<sup>2,3</sup>, Zizhao Ju<sup>1,2</sup>, Li Chen<sup>4</sup>, Li Zheng<sup>2,3</sup>, Jingjie Ge<sup>1,2</sup>, Xiaoniu Liang<sup>2,3</sup>, Weiqi Bao<sup>1,2</sup>, Ping Wu<sup>1,2</sup>, Ding Ding<sup>2,3</sup>, Tzu-Chen Yen<sup>5</sup>, Yihui Guan<sup>1,2\*</sup>, Chuantao Zuo<sup>1,2,6\*</sup> , Qianhua Zhao<sup>2,3,7\*</sup> and on behalf of the Shanghai Memory Study (SMS)

## Abstract

**Background** Gaining more information about the reciprocal associations between different biomarkers within the ATN (Amyloid/Tau/Neurodegeneration) framework across the Alzheimer's disease (AD) spectrum is clinically relevant. We aimed to conduct a comprehensive head-to-head comparison of plasma and positron emission tomography (PET) ATN biomarkers in subjects with cognitive complaints.

**Methods** A hospital-based cohort of subjects with cognitive complaints with a concurrent blood draw and ATN PET imaging (<sup>18</sup>F-florbetapir for A, <sup>18</sup>F-Florzolotau for T, and <sup>18</sup>F-fluorodeoxyglucose [<sup>18</sup>F-FDG] for N) was enrolled ( $n = 137$ ). The  $\beta$ -amyloid ( $A\beta$ ) status (positive versus negative) and the severity of cognitive impairment served as the main outcome measures for assessing biomarker performances.

**Results** Plasma phosphorylated tau 181 (p-tau181) level was found to be associated with PET imaging of ATN biomarkers in the entire cohort. Plasma p-tau181 level and PET standardized uptake value ratios of AT biomarkers showed a similarly excellent diagnostic performance for distinguishing between  $A\beta+$  and  $A\beta-$  subjects. An increased tau burden and glucose hypometabolism were significantly associated with the severity of cognitive impairment in  $A\beta+$  subjects. Additionally, glucose hypometabolism – along with elevated plasma neurofilament light chain level – was related to more severe cognitive impairment in  $A\beta-$  subjects.

**Conclusion** Plasma p-tau181, as well as <sup>18</sup>F-florbetapir and <sup>18</sup>F-Florzolotau PET imaging can be considered as interchangeable biomarkers in the assessment of  $A\beta$  status in symptomatic stages of AD. <sup>18</sup>F-Florzolotau and <sup>18</sup>F-FDG PET imaging could serve as biomarkers for the severity of cognitive impairment. Our findings have implications for establishing a roadmap to identifying the most suitable ATN biomarkers for clinical use.

**Keywords** ATN biomarkers, PET imaging, Plasma, Clinical severity

<sup>†</sup>Jiaying Lu and Xiaoxi Ma contributed equally to this work.

\*Correspondence:

Yihui Guan

guanyihui@hotmail.com

Chuantao Zuo

zuochuantao@fudan.edu.cn

Qianhua Zhao

qianhuazhao@fudan.edu.cn

Full list of author information is available at the end of the article



## Introduction

With the increase of the aging population worldwide, cognitive impairment is posing a tremendous burden on our society. In addition to dementia [1], subjective cognitive decline (SCD) [2] and mild cognitive impairment (MCI) [3] are two stages of cognitive decline that frequently occur in advanced age. Alzheimer's disease (AD), the most common form of dementia, is a multifaceted disease with different pathological and mechanistic substrates. The biological definition of AD, that is, the ATN (Amyloid/Tau/Neurodegeneration) framework, aiming for more precise and early disease identification, has gained substantial attraction in research settings [4]. The ATN biomarkers come in three major forms: cerebrospinal fluid (CSF), plasma, and imaging biomarkers. The development of highly specific immunoassays for CSF and plasma biomarkers and recent advances in the field of positron emission tomography (PET) imaging have largely improved the diagnostic accuracy. Notably, there is accumulating evidence supporting complementary roles for different sets of biomarkers. For example, a rise of CSF or plasma tau species appears to precede abnormal tau PET imaging during the course of AD [5]. This calls for a better understanding of the reciprocal interrelationships between different biomarker matrices within the ATN framework. There is also an unmet need to standardize and validate a strategic roadmap for routine application of ATN biomarkers in memory clinics [6]. Meanwhile, the assessment of relationship between ATN biomarkers and cognitive symptoms (C) is important given that a clinical-biological rather than a purely biological diagnosis of AD is recommended in clinical settings [7].

In recent years, much has been learned on the diagnostic performances of traditional CSF and imaging A ( $\beta$ -amyloid [ $A\beta$ ] PET, CSF  $A\beta_{42}$ , and CSF  $A\beta_{42}/A\beta_{40}$  ratio), T (tau PET and CSF phosphorylated tau [p-tau]), and N (anatomic magnetic resonance imaging [MRI],  $^{18}\text{F}$ -fluorodeoxyglucose [ $^{18}\text{F}$ -FDG] PET, and CSF total tau [t-tau]) biomarkers [4, 7]. Although plasma as a potential source of ATN markers has been increasingly explored to reduce the use of invasive lumbar punctures [8], much validation work remains to be done. Regarding the association between fluid and imaging biomarkers, CSF ( $A\beta_{42}$  for A, p-tau for T, neurofilament light chain [NfL] for N) and imaging ( $^{18}\text{F}$ -flutemetamol PET for A,  $^{18}\text{F}$ -flortaucipir PET for T, anatomic MRI for N) biomarkers are reported to be not interchangeable and the optimal approach varies by clinical stage [9]. Recently, plasma p-tau biomarkers (p-tau181, p-tau217, p-tau231) have been suggested to be valid indicators of amyloid and tau PET in clinical and community populations [10–16], although multiple comorbidities may affect the

interpretation of these biomarkers [16]. Meanwhile, similar to the non-commutable correlations between CSF and imaging biomarkers, plasma p-tau (p-tau181, p-tau217, p-tau231) and tau PET ( $^{18}\text{F}$ -flortaucipir,  $^{18}\text{F}$ -RO948,  $^{18}\text{F}$ -MK6240) biomarkers are thought to reflect different stages of tau pathology progression [17–19].

In this study, we present a comprehensive head-to-head comparison of plasma ( $A\beta_{42}/A\beta_{40}$  for A, p-tau181 for T, as well as NfL and t-tau for N) and PET imaging ( $^{18}\text{F}$ -florbetapir for A,  $^{18}\text{F}$ -Florzolotau for T, and  $^{18}\text{F}$ -FDG for N) ATN biomarkers in a hospital-based cohort of patients with cognitive complaints admitted to a memory clinic. The  $A\beta$  status (positive *versus* negative) and the severity of cognitive impairment served as the main outcome measures for assessing biomarker performances. The four plasma biomarkers included in the current study are relatively well-established and more readily available than other newly developed ones. The FDA-approved amyloid radiotracer  $^{18}\text{F}$ -florbetapir plays a cornerstone role in the diagnosis of AD [20]. The second-generation tau ligand  $^{18}\text{F}$ -Florzolotau (also known as  $^{18}\text{F}$ -APN-1607 or  $^{18}\text{F}$ -PM-PBB3) could overcome the limitations of first-generation tau PET tracers and reduce off-target binding [21].  $^{18}\text{F}$ -FDG is the most used PET tracer in nuclear medicine and its accessibility is significantly higher than that of any A and T PET imaging. The current study therefore provides a deeper insight into the comparability of plasma and PET imaging ATN biomarkers, which may be helpful for clinical and research applications. The outstanding strengths of the current study were that all participants were consecutively recruited from a real-life memory clinic, and the aforementioned biomarkers were available to all participants.

## Methods

### Participants

All procedures and visits occurred at the Memory Clinic of the Department of Neurology, Huashan Hospital, Fudan University (Shanghai, China) and the study was conducted as part of the hospital-based Shanghai Memory Study (SMS) [22]. Patients consecutively enrolled in the SMS were considered eligible if they presented with cognitive complaints and agreed on venous blood sampling ( $n=260$ ). After exclusion of subjects who refused multiple PET examinations due to radiation concerns ( $n=114$ ), the remaining 146 patients underwent assessment of PET ATN biomarkers using three different tracers ( $^{18}\text{F}$ -florbetapir for A,  $^{18}\text{F}$ -Florzolotau for T, and  $^{18}\text{F}$ -FDG for N). After the additional exclusion of patients who had contraindications to structural MRI ( $n=9$ ), the final population of interest consisted of 137 subjects. The study participants were finally categorized as being either  $A\beta$ -positive ( $A\beta+$ ) or  $A\beta$ -negative ( $A\beta-$ ) as described

below. A flowchart of patient recruitment is shown in Additional file 1: Figure S1. Variables collected for all participants included age, sex, years of education, and the presence of at least one apolipoprotein E (*APOE*)  $\epsilon 4$  allele.

### Diagnostic criteria

All clinical diagnoses were reached by consensus, following clinical interview and review of neuropsychological and biomarker data. Dementia was diagnosed according to the DSM-IV criteria [23], whereas the diagnosis of MCI was made according to the Petersen's criteria [3]. When a subject did not meet the criteria for MCI or any dementia but reported subjective experience of cognitive decline on one or more cognitive domains, an SCD label was assigned [24]. The clinical diagnosis of AD was based on the NINCDS-ADRDA criteria [25] along with A $\beta$  PET findings [4]. According to the ATN framework [4], all participants with positive findings in  $^{18}\text{F}$ -florbetapir amyloid PET (A $\beta$ +) were within the AD spectrum (cognitive impairment due to AD) while those with negative findings (A $\beta$ -) were ruled out from the AD continuum (cognitive impairment not due to AD).

### Evaluation of cognitive impairment severity

Clinical Dementia Rating (CDR) is a semi-structured inventory covering six cognitive, behavioral, and functional aspects. The neurologists need to score each of the above aspects with reference to information collected from participants and proxy. The global CDR score was calculated and the severity of cognitive impairment was assessed using a 5-point scale (0, 0.5, 1.0, 2.0, and 3.0) based on the Washington University CDR-assignment algorithm, with higher levels indicating higher severity [26, 27].

### Neuropsychological testing

The study participants underwent extensive neuropsychological testing to assess global cognition, instrumental activities of daily living, as well as memory, visuospatial, language, attention, and executive functions. Global cognition was assessed using the Mini-Mental State Examination (MMSE) and the Montreal Cognitive Assessment (MOCA). Instrumental activities of daily living were investigated using the Functional Assessment Questionnaire (FAQ) questionnaire. Raw scores of the Auditory Verbal Learning Test, Rey-Osterrieth Complex Fig test, Boston Naming Test, Trail Making Test, Clock Drawing Test, Verbal Fluency Test, Symbol Digit Modalities Test, and Similarity Test were collected and Z-transformed based on previously reported normative data [28]. Z-scores for each test were grouped according to specific cognitive domains (i.e., memory, visuospatial function,

language, attention, and executive functions) and averaged for subsequent analyses [28].

### Quantification of plasma ATN biomarkers

Whole blood collected into spray-coated  $\text{K}_2\text{EDTA}$  tubes was centrifuged at 1000 rpm for 15 min at 4 °C. The plasma fraction was transferred to a new 1.5-ml tube (Eppendorf, Hamburg, Germany) and stored at -80 °C until use. Plasma levels of A $\beta_{40}$  (A), A $\beta_{42}$  (A), p-tau181 (T), t-tau (N), and NfL (N) were measured simultaneously on a Simoa<sup>®</sup> HDx analyzer (Quanterix, Billerica, MA), according to the manufacturer's instructions. The A $\beta_{42}$ /A $\beta_{40}$  ratio was subsequently determined and used as the plasma A $\beta$  biomarker (A). Laboratory personnel were blinded to clinical information and imaging data. A detailed protocol has been reported elsewhere [29].

### Image acquisition

The mean (standard deviation) interval from PET imaging to blood collection was 2.6 (5.0) weeks. PET imaging ATN biomarkers were assessed using the following tracers:  $^{18}\text{F}$ -florbetapir for A ( $^{18}\text{F}$ -AV-45; 50–70 min post-injection),  $^{18}\text{F}$ -Florzolotau for T (90–110 min post-injection), and  $^{18}\text{F}$ -FDG for N (60–70 min post-injection). Static images were acquired on different days on a Biograph mCT Flow PET/CT system (Siemens, Erlangen, Germany). High-resolution structural MRI images obtained with a 3.0-T horizontal magnet scanner (Discovery MR750; GE Medical Systems, Milwaukee, WI) were used for spatial normalization. The protocols used for acquisition have been described previously in detail [30–32].

### Assessment and classification of A $\beta$ PET images

Raw A $\beta$  PET images were visually interpreted using dedicated software (Siemens syngo.via) by two independent neuroradiologists (CZ, more than 20 years of experience; JL, more than 5 years of experience) blinded to clinical and laboratory data. Each participant was classified as either A $\beta$ -positive (A $\beta$ +) or A $\beta$ -negative (A $\beta$ -) according to the criteria proposed previously [33]. A third expert (HZ, more than 10 years of experience) was invited to review images in case of discrepancies; the final classification was based on majority voting.

### Image processing and semi-quantitative analysis

Images were processed via Statistical Parametric Mapping 12 (SPM12; <http://www.fil.ion.ucl.ac.uk/spm/software/spm12/>) implemented in MATLAB (version 2018b, MathWorks, Natick, MA). Prior to smoothing (full-width at half-maximum: 8 mm), raw PET images were first co-registered to the concurrent structural MRI images and then spatially normalized to the Montreal Neurological

Institute standard space using the transformation matrices of segmented individual structural MRI images. The following reference regions were selected: whole cerebellum for  $^{18}\text{F}$ -florbetapir PET [34], cerebellar grey matter for  $^{18}\text{F}$ -Florzolotau PET [31], and pons for  $^{18}\text{F}$ -FDG PET [35]. Standardized uptake value ratio (SUVR) images were obtained after reference region-based intensity normalization.  $\text{A}\beta$  SUVR values were quantified in the following regions of interest (ROIs) defined according to the Automated Anatomical Labelling Atlas three (AAL3) [36]: bilateral frontal lobes, anterior cingulate gyrus, posterior cingulate gyrus, lateral parietal gyrus and lateral temporal gyrus. In accordance with previous methodology [34], the unweighted average SUVR value of the ROIs located above was considered as the global  $\text{A}\beta$  SUVR. Tau SUVR values were determined in the following ROIs according to the Desikan-Killiany Atlas [37]: bilateral entorhinal cortex, amygdala, middle temporal gyrus, and inferior temporal gyrus. In keeping with a previous study [38], the unweighted average SUVR value of the first two ROIs and the weighted average SUVR value of the last two ROIs were considered as the medial temporal lobe (MTL) and temporal neocortex (NEO-T) SUVR values for tau, respectively.  $^{18}\text{F}$ -FDG SUVR values were quantified in the following ROIs defined according to the AAL3 [36]: bilateral angular gyri, posterior cingulate gyrus, and inferior temporal gyrus. The unweighted average SUVR value of all ROIs was considered as the meta-analytically derived region of interest (metaROI) SUVR for determining an abnormal glucose metabolic activity [39].

### Statistics

The Kolmogorov–Smirnov test was used to test the normal distribution of continuous variables. Intergroup comparisons between  $\text{A}\beta+$  and  $\text{A}\beta-$  subjects were performed using independent Student's *t*-tests (normally distributed continuous variables), Mann–Whitney *U* tests (skewed continuous variables), and chi-square tests (categorical variables), as appropriate. The reciprocal associations between plasma and PET imaging ATN biomarkers were investigated at both voxel and region levels. For voxel-wise analysis, the multiple regression model implemented in SPM12 was applied to the entire cohort, as well as separately to  $\text{A}\beta+$  and  $\text{A}\beta-$  subjects. Age, sex, and the interval from PET imaging to blood collection (expressed in weeks) were entered as covariates, with the statistical threshold being set at a family wise error (FWE)-corrected *P* value ( $P_{\text{FWE}} < 0.05$ ). For region-level assessments, partial correlation analysis after adjustment for age, sex, and the interval from PET imaging to blood collection was applied to the entire cohort, as well as separately to  $\text{A}\beta+$  and  $\text{A}\beta-$  subjects. Generalized linear models (GLMs) adjusted for age and sex were used

to compare the performances of plasma and PET imaging ATN biomarkers in  $\text{A}\beta+$  and  $\text{A}\beta-$  subjects. The ability of biomarkers in distinguishing the  $\text{A}\beta$  status was determined by receiver operating characteristic (ROC) curve analysis. Agreement and Cohen's kappa were calculated to assess the concordance between biomarkers. The optimal cutoff values for biomarker-based classification were determined with the greatest Youden's index based on the ROC curve analysis. The associations between plasma and PET imaging ATN biomarkers and the severity of cognitive impairment (CDR scores) were investigated using GLMs adjusted for age and sex in the entire cohort, as well as separately to  $\text{A}\beta+$  and  $\text{A}\beta-$  subjects. Finally, age- and sex-adjusted partial correction analysis was implemented to investigate the correlations between biomarkers and the results of neuropsychological testing. Data were analyzed using SPSS, version 23 (IBM, Armonk, NY), unless otherwise indicated. Bonferroni-corrected *P* values ( $P_c$ ) were used to adjust for multiple comparisons. Two-tailed *P* values  $< 0.05$  were considered statistically significant, unless otherwise indicated. Further adjustments for education and *APOE*  $\epsilon 4$  were also made for all analysis where applicable and relevant results are presented in Additional file 1: Fig. S2, Fig. S4–S6, Table S1–S4.

## Results

### Participants

The final study cohort consisted of 137 patients with cognitive complaints who were classified as either  $\text{A}\beta$ -positive ( $\text{A}\beta+$ ;  $n=90$ ) or  $\text{A}\beta$ -negative ( $\text{A}\beta-$ ;  $n=47$ ) based on visual interpretation of  $^{18}\text{F}$ -florbetapir PET imaging findings. The  $\text{A}\beta+$  group comprised 29 patients with MCI due to AD and 61 with AD dementia, whereas the  $\text{A}\beta-$  group included 10 subjects with SCD, 26 patients with MCI not due to AD and 11 with dementia not due to AD. There were no intergroup differences in terms of age, years of education, and interval from PET imaging to blood collection (Table 1); however, the  $\text{A}\beta+$  group showed more severe cognitive impairment and included a higher proportion of women and *APOE*  $\epsilon 4$  allele-carriers.

### Reciprocal associations between plasma and PET imaging ATN biomarkers

The reciprocal associations between plasma and PET imaging ATN biomarkers analyzed on a voxel-wise level ( $P_{\text{FWE}} < 0.05$ ) are shown in Fig. 1. In the entire cohort, the plasma p-tau181 level showed positive correlations with (1)  $\text{A}\beta$  PET SUVR value throughout the entire cortex – with only exception in the MTL as well as the precentral and postcentral gyrus (Fig. 1a) and (2) tau PET SUVR value throughout the entire cortex, with exception

**Table 1** General characteristics of the study participants stratified according to the A $\beta$  status

	A $\beta$ + subjects	A $\beta$ - subjects	P value
Number of subjects	90	47	–
Age, years	65.5 (9.6)	66.1 (7.9)	0.696 <sup>a</sup>
Sex, female, %	61.1	42.6	0.047 <sup>b</sup>
Education, years	10.6 (3.9)	11.7 (4.6)	0.165 <sup>a</sup>
APOE $\epsilon$ 4 carriers, % <sup>e</sup>	61.8	21.3	<0.001 <sup>b</sup>
Interval from PET imaging to blood collection, weeks	2.3 (4.6)	3.2 (5.6)	0.318 <sup>a</sup>
<i>Neuropsychological tests</i>			
CDR, number of subjects	CDR=0, 0 CDR=0.5, 29 CDR=1, 45 CDR=2, 13 CDR=3, 3	CDR=0, 8 CDR=0.5, 30 CDR=1, 6 CDR=2, 3 CDR=3, 0	<0.001 <sup>c*</sup>
MMSE	22.0 [19.0, 25.0]	26.0 [24.0, 28.0]	<0.001 <sup>c*</sup>
MOCA <sup>e</sup>	16.0 [9.5, 19.0]	19.0 [16.0, 24.0]	<0.001 <sup>c*</sup>
FAQ	12.5 [8.8, 18.0]	7.0 [4.0, 9.0]	<0.001 <sup>c*</sup>
Memory <sup>e,f</sup>	– 2.1 [– 2.5, – 1.7]	– 1.6 [– 2.1, – 0.6]	<0.001 <sup>c*</sup>
Visuospatial function <sup>e,f</sup>	– 1.7 [– 6.9, 0.1]	0.0 [– 2.4, 0.7]	0.002 <sup>c*</sup>
Language <sup>e,f</sup>	– 1.6 [– 2.8, – 0.6]	– 0.9 [– 1.7, – 0.2]	0.004 <sup>c*</sup>
Attention <sup>e,f</sup>	– 2.1 [– 6.3, – 0.6]	– 0.7 [– 1.4, 0.0]	<0.001 <sup>c*</sup>
Executive function <sup>e,f</sup>	– 3.8 [– 10.1, – 1.3]	0.1 [– 2.5, 2.5]	<0.001 <sup>c*</sup>
<i>PET ATN biomarkers</i>			
A: Global SUVR	1.4 [1.3, 1.5]	1.2 [1.1, 1.2]	<0.001 <sup>d*</sup>
T: MTL SUVR	1.6 [1.4, 1.8]	1.1 [1.0, 1.2]	<0.001 <sup>d*</sup>
T: NEO-T SUVR	1.5 [1.3, 1.8]	1.0 [1.0, 1.1]	<0.001 <sup>d*</sup>
N: metaROI SUVR	1.2 [1.1, 1.4]	1.4 [1.4, 1.6]	<0.001 <sup>d*</sup>
<i>Plasma ATN biomarkers</i>			
A: A $\beta$ <sub>42</sub> /A $\beta$ <sub>40</sub> ratio	0.04 [0.04, 0.06]	0.05 [0.04, 0.06]	0.054 <sup>d</sup>
T: P-tau181, pg/ml	4.8 [3.9, 6.0]	2.5 [1.8, 2.9]	<0.001 <sup>d*</sup>
N: T-tau, pg/ml	3.4 [2.3, 5.4]	3.2 [2.1, 4.6]	0.238 <sup>d</sup>
N: NfL, pg/ml	18.0 [14.5, 21.6]	13.6 [8.8, 20.7]	0.064 <sup>d</sup>

Data are presented as mean (standard deviation) or median [quartile 1, quartile 3], unless otherwise indicated

Each participant was classified as either A $\beta$ -positive (A $\beta$ +) or A $\beta$ -negative (A $\beta$ -) based on <sup>18</sup>F-florbetapir PET imaging findings. Unadjusted P values are presented, and those surviving multiple comparisons (Bonferroni's correction,  $P_c < 0.05$ ) are marked with an asterisk (\*)

<sup>a</sup>Independent Student's t-test. <sup>b</sup>Chi-square test. <sup>c</sup>Mann-Whitney U test. <sup>d</sup>Generalized linear model adjusted for age and sex. <sup>e</sup>One patient had missing data. <sup>f</sup>Z-score transformed

APOE Apolipoprotein E, PET Positron emission tomography, CDR Clinical Dementia Rating, MMSE Mini-Mental State Examination, MOCA Montreal Cognitive Assessment, FAQ Functional Activities Questionnaire, A/T/N Amyloid/Tau/Neurodegeneration, SUVR Standardized uptake value ratio, MTL medial temporal lobe, NEO-T Temporal neocortex, metaROI Meta-analytically derived region of interest, t-tau Total tau, NfL Neurofilament light chain

in the precentral and postcentral gyrus (Fig. 1b). Therefore, the findings of A $\beta$  and tau PET imaging in the MTL differed significantly. Besides, the strength of the associations was lower for A $\beta$  PET compared with tau PET imaging. On analyzing the <sup>18</sup>F-FDG PET data, the plasma p-tau181 level was negatively correlated with SUVR values measured in the angular gyrus, precuneus, inferior parietal gyrus, as well as middle and posterior cingulate gyrus (Fig. 1c). No other significant associations between plasma and PET imaging ATN biomarkers were observed in the entire study cohort. In addition, all correlation

analyses yielded negative results when A $\beta$ + and A $\beta$ - patients were separately considered (Fig. 1). On a region-level basis (Table 2), the results were largely similar to those observed at the voxel-level. Consistent findings were seen when further adjusted for education and APOE  $\epsilon$ 4 (Additional file 1: Fig. S2, Table S1).

#### Plasma and PET imaging ATN biomarkers in relation to the A $\beta$ status

Compared with A $\beta$ - participants, the A $\beta$ + participants consistently showed an increased pathological burden

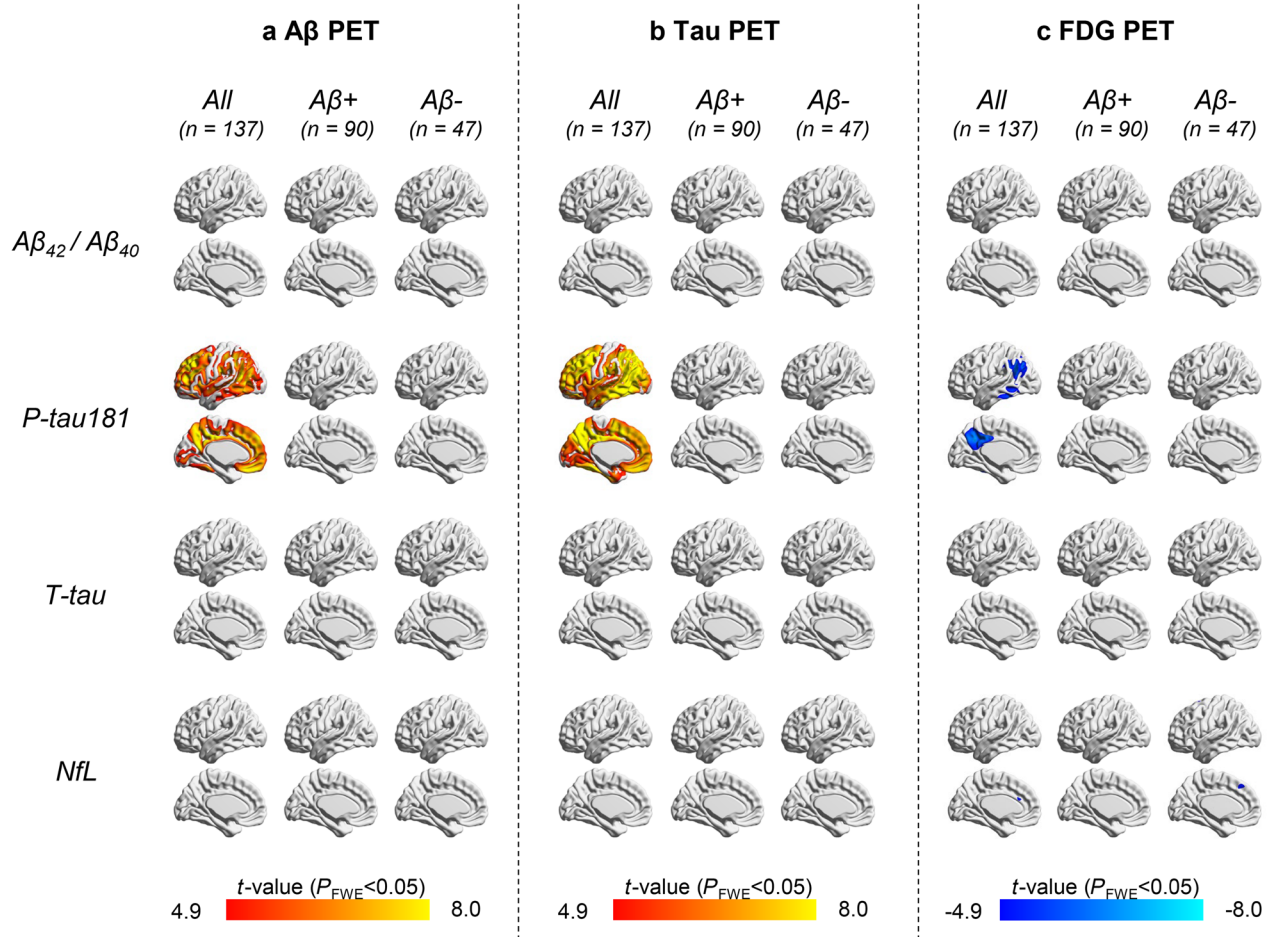


**Fig. 1** Reciprocal associations between plasma and PET imaging ATN biomarkers: voxel-wise analysis. Voxel-wise regression analysis of standardized uptake value ratios from  $^{18}\text{F}$ -florbetapir PET for A (a),  $^{18}\text{F}$ -Florizotau PET for T (b), and  $^{18}\text{F}$ -FDG PET for N (c) in relation to plasma ATN biomarkers ( $\text{A}\beta_{42}/\text{A}\beta_{40}$  ratio, p-tau181, t-tau, NfL) adjusted for age, sex, and the interval from PET imaging to blood collection; calculations were performed in the entire cohort, as well as in  $\text{A}\beta+$  and  $\text{A}\beta-$  subjects. The statistical threshold was set at a family wise error (FWE)-corrected  $P$  value  $< 0.05$ . The positive correlations are displayed in orange-red color scale. The negative correlations are displayed in cyan-blue color scale. PET Positron emission tomography, t-tau, total tau, NfL Neurofilament light chain, FWE Family-wise error

as reflected by higher PET SUVR values for AT biomarkers and lower PET SUVR value for N biomarker ( $P_c < 0.001$ ; Table 1). Similar findings were observed for plasma biomarkers, with significantly higher p-tau181 level ( $P_c < 0.001$ ) and a trend towards lower  $\text{A}\beta_{42}/\text{A}\beta_{40}$  ratio ( $P = 0.054$ ) and higher NfL level ( $P = 0.064$ ) in the  $\text{A}\beta+$  participants. However, plasma t-tau concentrations showed no intergroup difference. When further adjusted for education and *APOE*  $\epsilon 4$  status, the differences in all PET biomarkers and plasma p-tau remained between  $\text{A}\beta+$  and  $\text{A}\beta-$  subjects ( $P_c < 0.001$ ) and there was still no difference in plasma t-tau ( $P = 0.308$ ); however, the difference in plasma NfL reached the level of statistical significance ( $P_c < 0.039$ ).

On analyzing the areas under the ROC curve (AUC) for distinguishing between  $\text{A}\beta+$  and  $\text{A}\beta-$  subjects (Table 3), we found excellent diagnostic performances of the following biomarkers: global SUVR value for A (AUC=0.93), MTL SUVR value for T (AUC=0.94), NEO-T SUVR value for T (AUC=0.95), and plasma p-tau181 level for T (AUC=0.93). The accuracy of the metaROI SUVR value for N was less remarkable (AUC=0.83), whereas plasma biomarkers for A and N lacked discriminatory ability (AUC  $\leq 0.65$ ). We next examined the agreement between plasma and PET imaging ATN biomarkers that were found to distinguish between  $\text{A}\beta+$  and  $\text{A}\beta-$  patients. As expected (Fig. 2), plasma p-tau181 level for T and PET SUVR value for T

**Table 2** Region-level reciprocal associations between plasma and PET imaging ATN biomarkers

	A A $\beta_{42}$ /A $\beta_{40}$ ratio		T p-tau181, pg/ml		N t-tau, pg/ml		N NfL, pg/ml	
	<i>r</i>	<i>P</i>	<i>r</i>	<i>P</i>	<i>r</i>	<i>P</i>	<i>r</i>	<i>P</i>
<i>Entire cohort (n = 137)</i>								
A: Global SUVR	-0.044	0.617	0.528	<b>&lt;0.001***</b>	0.039	0.653	0.036	0.679
T: MTL SUVR	-0.018	0.836	0.613	<b>&lt;0.001***</b>	0.078	0.373	0.172	<b>0.046</b>
T: NEO-T SUVR	-0.035	0.686	0.623	<b>&lt;0.001***</b>	0.081	0.350	0.204	<b>0.018</b>
N: metaROI SUVR	0.026	0.767	-0.491	<b>&lt;0.001***</b>	-0.013	0.885	-0.189	<b>0.029</b>
<i>A<math>\beta</math>+ (n = 90)</i>								
A: Global SUVR	0.070	0.520	0.143	0.186	-0.046	0.669	-0.044	0.683
T: MTL SUVR	0.122	0.259	0.254	<b>0.018</b>	-0.047	0.665	0.063	0.563
T: NEO-T SUVR	0.123	0.257	0.274	<b>0.010</b>	-0.043	0.693	0.142	0.188
N: metaROI SUVR	-0.146	0.178	-0.217	<b>0.043</b>	0.171	0.112	-0.042	0.700
<i>A<math>\beta</math>- (n = 47)</i>								
A: Global SUVR	0.187	0.223	0.242	0.113	-0.094	0.545	-0.260	0.089
T: MTL SUVR	0.324	<b>0.032</b>	0.362	<b>0.016</b>	-0.108	0.484	0.090	0.561
T: NEO-T SUVR	0.220	0.151	0.380	<b>0.011</b>	-0.102	0.509	0.062	0.691
N: metaROI SUVR	-0.013	0.931	-0.033	0.831	0.032	0.838	-0.239	0.118

Partial correction analysis adjusted for age, sex, and the interval from PET imaging to blood collection was undertaken to assess the reciprocal associations between plasma and PET imaging ATN biomarkers. The reported *P* values are unadjusted. Significant *P* values (*P* < 0.05) are marked in bold, those surviving multiple comparisons (Bonferroni's correction) are marked with asterisks (\*\*\*, *P*<sub>c</sub> < 0.001)

PET Positron emission tomography, A/T/N Amyloid/Tau/Neurodegeneration, SUVR Standardized uptake value ratio, MTL Medial temporal lobe, NEO-T Temporal neocortex, metaROI Meta-analytically derived region of interest, t-tau Total tau, NfL Neurofilament light chain

**Table 3** Performance of plasma and PET imaging ATN biomarkers for predicting the A $\beta$  status

	AUC (95% CI)	<i>P</i> value	Sensitivity (%)	Specificity (%)	Optimal cutoff
<i>PET ATN biomarkers</i>					
A: Global SUVR	0.93 (0.88–0.97)	<b>&lt;0.001***</b>	86.7	89.4	1.25
T: MTL SUVR	0.94 (0.82–0.96)	<b>&lt;0.001***</b>	82.2	95.7	1.30
T: NEO-T SUVR	0.95 (0.91–0.99)	<b>&lt;0.001***</b>	86.7	97.9	1.23
N: metaROI SUVR	0.83 (0.76–0.90)	<b>&lt;0.001***</b>	80.9	72.2	1.37
<i>Plasma ATN biomarkers</i>					
A: A $\beta_{42}$ /A $\beta_{40}$ ratio	0.63 (0.54–0.73)	<b>0.011</b>	80.9	45.6	0.04
T: P-tau181, pg/ml	0.93 (0.88–0.98)	<b>&lt;0.001***</b>	93.3	85.1	3.23
N: T-tau, pg/ml	0.56 (0.46–0.66)	0.265	17.8	97.9	5.76
N: NfL, pg/ml	0.65 (0.54–0.75)	<b>0.005*</b>	81.1	51.1	13.63

Each participant was classified as either A $\beta$ -positive (A $\beta$ +) or A $\beta$ -negative (A $\beta$ -) based on <sup>18</sup>F-florbetapir PET imaging findings. Each plasma and PET imaging ATN biomarker was examined by receiver operating characteristic (ROC) curve analysis in relation to its ability to predict the A $\beta$  status. The optimal cutoff for each biomarker was selected as the point that maximized the Youden's index according to the ROC curve analysis; the corresponding sensitivity and specificity were subsequently calculated. Unadjusted *P* values are presented. Significant *P* values (*P* < 0.05) are marked in bold, and those surviving multiple comparisons (Bonferroni's correction) are marked with asterisks (\*\*\*, *P*<sub>c</sub> < 0.001; \*, *P*<sub>c</sub> < 0.05)

PET Positron emission tomography, A/T/N Amyloid/Tau/Neurodegeneration, SUVR Standardized uptake value ratio, MTL Medial temporal lobe, NEO-T Temporal neocortex, metaROI meta-analytically derived region of interest, p-tau181 Tau phosphorylated at threonine 181, t-tau Total tau, NfL Neurofilament light chain, AUC Area under the curve, CI Confidence interval

showed a fairly high agreement (plasma p-tau181 level versus MTL SUVR value for T: Cohen's kappa = 0.65; plasma p-tau181 level versus NEO-T SUVR value for T: Cohen's kappa = 0.72). In addition, plasma p-tau181 level for T showed moderate agreement with both PET SUVR value for A (Cohen's kappa = 0.59) and PET

SUVR value for N (Cohen's kappa = 0.45). Additional file 1: Fig. S3 shows a pairwise analysis of the observed agreement between different PET imaging ATN biomarkers – which ranged from substantial (A and T: Cohen's kappa = 0.61 [global SUVR value for A versus MTL SUVR value for T], 0.70 [global SUVR value for

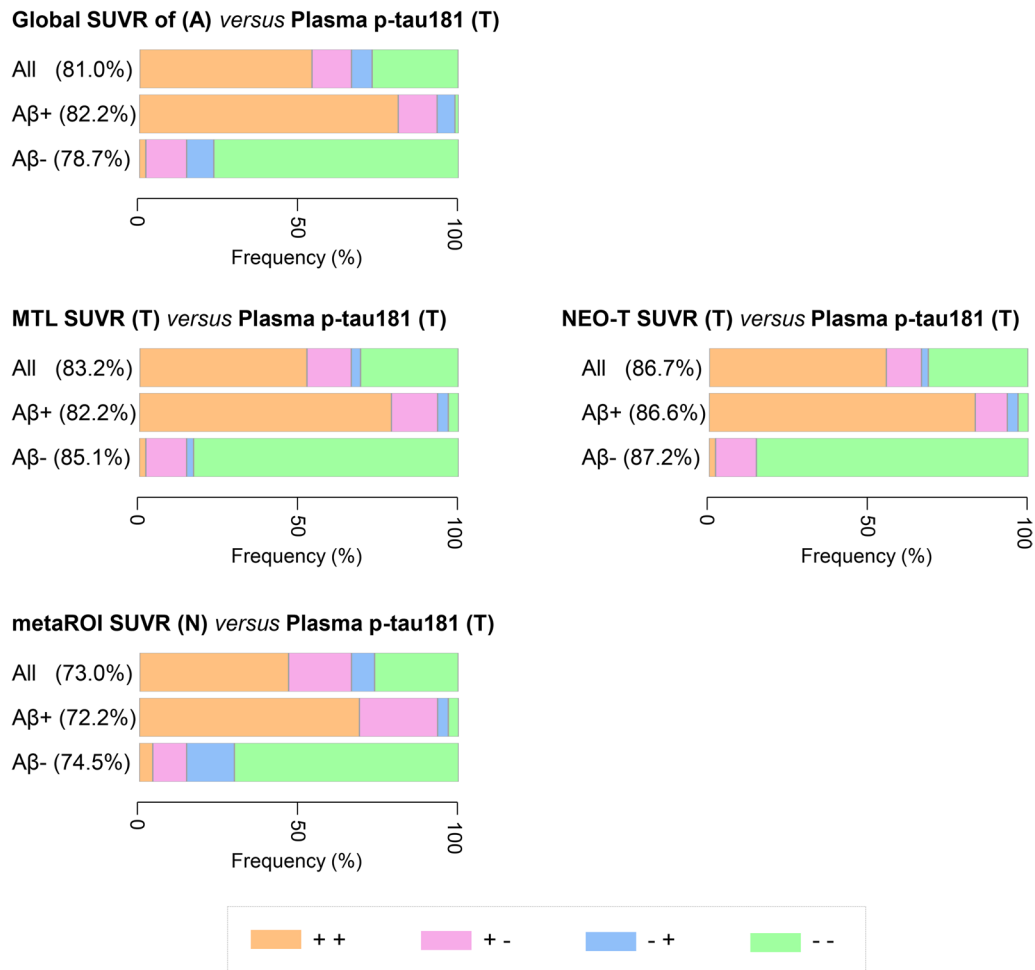


**Fig. 2** Agreement between plasma p-tau181 levels and PET imaging ATN biomarkers for predicting the Aβ status. The concordance rates are based on the established thresholds for the biomarkers. The sums of negative and positive concordance rates are presented. Color bars summarize the concordance rates between plasma p-tau181 level and different PET imaging ATN biomarkers in the entire cohort (upper row) as well as Aβ+ subjects (intermediate row) and Aβ- subjects (lower row). Negative (– –) and positive (+ +) agreement are denoted in green and orange, respectively. Disagreement is reported in magenta (+ –; positive SUVR value on PET and negative p-tau181 level) or in blue (– +; negative SUVR value on PET and positive p-tau181 level). A/T/N, Amyloid/Tau/Neurodegeneration, SUVR Standardized uptake value ratio, MTL Medial temporal lobe, NEO-T Temporal neocortex; metaROI, meta-analytically derived region of interest; p-tau181, tau phosphorylated at threonine 181

A versus NEO-T SUVR value for T) to moderate (T and N: Cohen’s kappa = 0.48 [NEO-T SUVR value for T versus metaROI SUVR value for N], 0.50 [MTL SUVR value for T versus metaROI SUVR value for N]) and fair (A and N: Cohen’s kappa = 0.33).

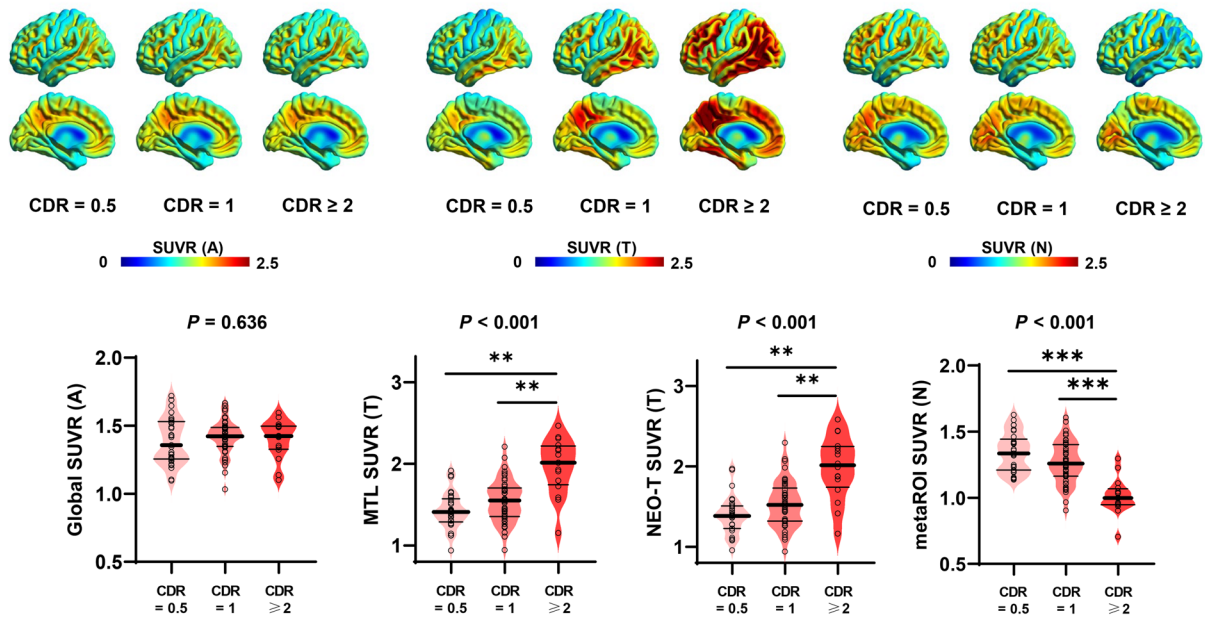
**Plasma and PET imaging ATN biomarkers in relation to the severity of cognitive impairment**

We next analyzed plasma and PET imaging ATN biomarkers in relation to the severity of cognitive impairment; to this aim, the study participants were categorized in different CDR categories.

The Aβ+ subjects were divided into three categories (CDR = 0.5, n = 29; CDR = 1, n = 45; CDR ≥ 2,

n = 16). Group-average SUVR maps for each CDR category are presented in Fig. 3a. MTL SUVR value for T, NEO-T SUVR value for T and metaROI SUVR value for N showed that the tau burden increased and the glucose metabolism decreased in a stepwise fashion with increased CDR. Neither global SUVR value for A (Fig. 3a) nor plasma ATN biomarkers (Fig. 3b) showed such associations. On analyzing Aβ- subjects, we found that the CDR categories did not show significant associations with either plasma or PET imaging ATN biomarkers (Additional file 1: Fig. S4), with the only exceptions being metaROI SUVR value and plasma NfL level (both for N). Specifically, glucose hypometabolism showed a trend towards a higher frequency

**a PET biomarkers**



**b Plasma biomarkers**

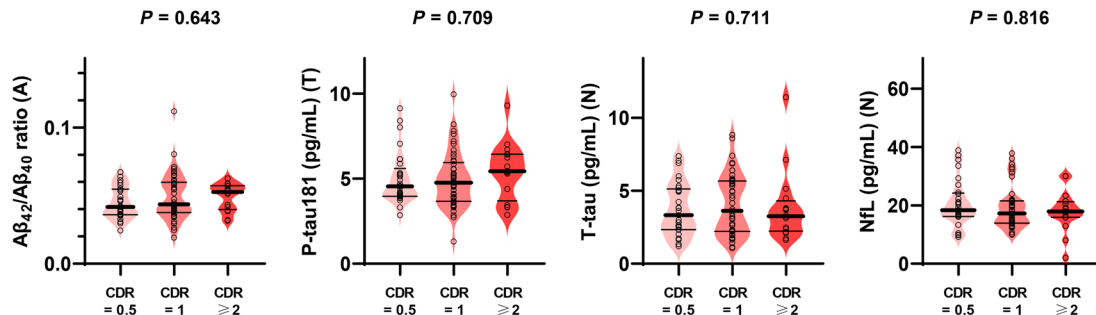


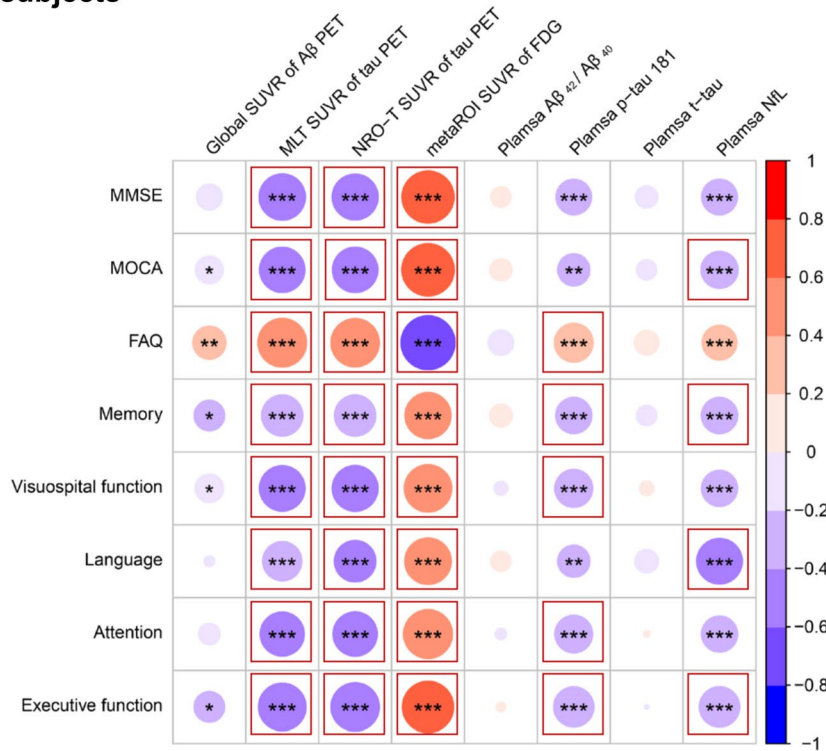
**Fig. 3** Plasma and PET imaging ATN biomarkers in relation to the severity of cognitive impairment in  $A\beta+$  subjects. Average SUVR maps for PET imaging A (left), T (middle), and N (right) biomarkers in relation to different CDR categories (**a**; upper row). Generalized linear models after adjustment for age and sex were applied to analyze the values of PET (**a**; lower row) and plasma (**b**) ATN biomarkers in relation to the severity of cognitive impairment. Unadjusted  $P$  values are presented for differences between the three CDR categories, whereas those that remained significant after correcting for multiple comparisons (Bonferroni’s correction) are marked with asterisks (\*\*\*,  $P_c < 0.001$ ; \*\*,  $P_c < 0.01$ ). The thick solid line, the thin solid lines, and the dots denote the median, the 25th and 75th percentiles, and individual values, respectively. *CDR* Clinical Dementia Rating, *PET* Positron emission tomography, *ATN* Amyloid/Tau/Neurodegeneration, *SUVR* Standardized uptake value ratio, *MTL* Medial temporal lobe, *NEO-T* Temporal neocortex, *metaROI* Meta-analytically derived region of interest, *p-tau181* tau phosphorylated at threonine 181, *t-tau* total tau, *NfL* Neurofilament light chain

in patients with more severe cognitive impairment, although the difference did not persist after correcting for multiple comparisons. Plasma NfL level was significantly higher in patients with a  $CDR \geq 1$  than in those with a  $CDR = 0.5$  ( $P_c < 0.01$ ). The results from the entire cohort are shown in Additional file 1: Fig. S5. Similar results were obtained after corrections for education and *APOE*  $\epsilon 4$  status (Additional file 1: Tables S2-S4).

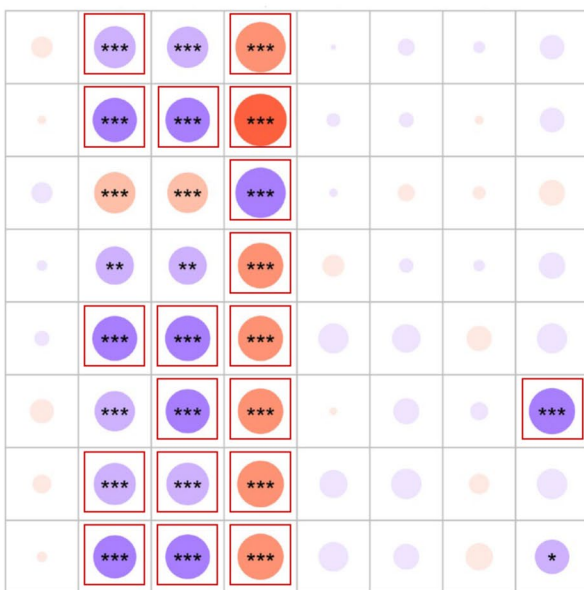
**Plasma and PET imaging ATN biomarkers in relation to neuropsychological tests**

On analyzing the entire study cohort, we found consistent associations between the results of neuropsychological tests and MTL SUVR value for T, NEO-T SUVR value for T, as well as metaROI SUVR value for N (Fig. 4a) – with statistical significance remaining after correcting for multiple comparisons. Similar significant associations were observed between plasma p-tau181 level for

**a All subjects**



**b Aβ+ subjects**



**c Aβ- subjects**

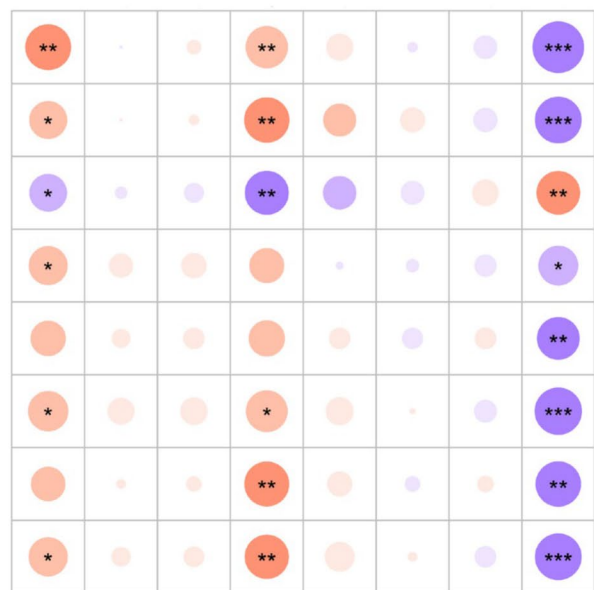


**Fig. 4** Associations of plasma and PET imaging ATN biomarkers with neuropsychological tests. Partial correlation analysis after adjustment for age and sex was applied to evaluate the associations between plasma and PET imaging ATN biomarkers and the results of neuropsychological tests in the entire cohort **(a)** as well as in Aβ+ **(b)** and Aβ- **(c)** subjects. Unadjusted *P* values are presented with asterisks (\*\*\*, *P* < 0.001; \*\*, *P* < 0.01; \*, *P* < 0.05) whereas those that remained significant after correcting for multiple comparisons (Bonferroni's correction, *P<sub>c</sub>* < 0.05) are marked with solid frames. The results of neuropsychological testing on different cognitive domains were transformed to Z-scores. The color bars denote partial correlation coefficients (*r*). *MMSE* Mini-Mental State Examination, *MOCA* Montreal Cognitive Assessment, *FAQ* Functional Activities Questionnaire, *PET* Positron emission tomography, *SUVR* Standardized uptake value ratio, *MTL* Medial temporal lobe; *NEO-T* Temporal neocortex, *metaROI* Meta-analytically derived region of interest, *t-tau* total tau, *NfL* Neurofilament light chain

T and the results of the FAQ, as well as memory, visuospatial function, attention, and executive functioning. The plasma NfL level for N was significantly associated with the results of MOCA, as well as memory, language, and executive functioning. The results in the A $\beta$ + group (Fig. 4b) were generally consistent with those obtained in the entire cohort. However, no significant associations were observed when ATN biomarkers were analyzed in relation to neuropsychological tests in A $\beta$ - subjects (Fig. 4c). Further corrections for education and *APOE*  $\epsilon$ 4 did not change the findings (Additional file 1: Fig. S6). The only exception was that in A $\beta$ - subjects, the nonsignificant associations between plasma NfL level and scores of neuropsychological tests reached the significance after further adjustment for education and *APOE*  $\epsilon$ 4.

## Discussion

The present study has three main findings. First, plasma p-tau181 level was found to be significantly associated with PET imaging ATN biomarkers in the entire study cohort, although this association did not persist when A $\beta$ + and A $\beta$ - subjects were analyzed separately. Second, we identified four biomarkers (global SUVR value for A, MTL SUVR value for T, NEO-T SUVR value for T, and plasma p-tau181 level for T) with similar and good performance in distinguishing between A $\beta$ + and A $\beta$ - subjects. Third, we found that an increasing tau burden (as reflected by higher MTL and NEO-T SUVR values on <sup>18</sup>F-Florzolotau PET) and a decreasing glucose metabolism (as reflected by lower metaROI SUVR value on <sup>18</sup>F-FDG PET) were significantly associated with the severity of cognitive impairment in A $\beta$ + subjects. Glucose hypometabolism, along with elevated plasma NfL level, was also related to more severe cognitive impairment in A $\beta$ - subjects. Taken together, while both <sup>18</sup>F-Florzolotau tau PET and plasma p-tau181 are interchangeable markers for <sup>18</sup>F-florbetapir amyloid PET on detecting the presence of amyloid pathology in unselected patients with cognitive complaints, plasma p-tau181 is preferred in screening considering the cost-effectiveness. Further, our study provides scoping information about the potential usefulness of <sup>18</sup>F-Florzolotau PET and <sup>18</sup>F-FDG PET as markers of clinical severity, and none of the plasma biomarkers included in the current study could be used interchangeably in this regard. Notably, since all participants had cognitive complaints and were recruited from a real-life memory clinic, the current findings may only apply to the symptomatic population.

In addition to the established imaging and CSF markers (A $\beta$  PET imaging and CSF A $\beta$ <sub>42</sub>/A $\beta$ <sub>40</sub> ratio) [40], plasma-based biomarkers have frequently been investigated for their ability to identify subjects with amyloid pathology – with most studies focusing on the plasma A $\beta$ <sub>42</sub>/A $\beta$ <sub>40</sub>

ratio. However, reliable studies have shown that the A $\beta$ <sub>42</sub>/A $\beta$ <sub>40</sub> ratio in plasma generally underperforms the established CSF and imaging A biomarkers [41] and is prone to significant analytical variation [42]. By relying on the visual interpretation of <sup>18</sup>F-florbetapir PET images to achieve a dichotomous classification of the A $\beta$  status, our current findings further support the view that the plasma A $\beta$ <sub>42</sub>/A $\beta$ <sub>40</sub> ratio has a limited value as an A biomarker [43]. Additionally, we found that neither plasma nor PET imaging A biomarkers were significantly associated with the severity of cognitive impairment. This finding is consistent with previous observations showing that cerebral A $\beta$  accumulation reaches a plateau during the prodromal stage [44] and that the plasma amyloid biomarker profile does not correlate with cognitive function across the clinical spectrum of AD [45].

The agreement between PET, CSF, and plasma T biomarkers varies widely from 66% to 95% [46] and can be influenced by differences in assays and laboratory procedures [47]. The association of plasma p-tau181 (T) with CSF p-tau181 (T) as well as <sup>18</sup>F-flortaucipir PET (T) and <sup>18</sup>F-flutemetamol PET (A) has been previously reported for A $\beta$ + subjects and for an unselected sample comprising both A $\beta$ + and A $\beta$ - individuals – but not for A $\beta$ - subjects analyzed separately [11]. These findings are also consistent with an analysis by Thijssen et al. who reported significant associations of <sup>18</sup>F-flortaucipir PET (T) with both plasma p-tau181 (T) and p-tau217 (T) [48]. In our study, associations of plasma p-tau181 (T) with <sup>18</sup>F-Florzolotau PET (T), <sup>18</sup>F-florbetapir PET (A), and <sup>18</sup>F-FDG PET (N) were examined. However, they reached the threshold for statistical significance only in the entire study cohort. On analyzing A $\beta$ + individuals separately, our results were not consistent with previous studies possibly because we included only subjects with MCI and dementia due to AD but not those in the preclinical stage, as other authors did [11, 48].

Our data also showed that the plasma p-tau181 level (T) was more closely associated with <sup>18</sup>F-Florzolotau PET (T) than <sup>18</sup>F-florbetapir PET (A), although Thijssen et al. found that the plasma p-tau biomarkers were mainly related to PET imaging A biomarkers (<sup>18</sup>F-AZD4694, <sup>18</sup>F-florbetapir) than T biomarkers (<sup>18</sup>F-MK6240, <sup>18</sup>F-flortaucipir) [48]. This discrepancy might be because that the present study used a different tau PET tracer (<sup>18</sup>F-Florzolotau) and did not include subjects in the preclinical stage. It is worth noting that <sup>18</sup>F-Florzolotau has shown favorable affinity to all types of tau aggregates [21] and is able to detect tau deposition in vivo in the brains of patients with different tauopathies (i.e., three- and four-repeat (3R/4R) tau in AD [49–51], 4R-tau in progressive supranuclear palsy [31, 52], 4R and 3R/4R-tau in frontotemporal lobar degeneration with tauopathy caused by

microtubule-associated protein tau mutations [53]) while  $^{18}\text{F}$ -MK6240 and  $^{18}\text{F}$ -flortaucipir have relatively low affinity for non-AD tauopathies [54–56].

Plasma levels of p-tau biomarkers have been reported to be strongly correlated with both CSF and PET imaging T biomarkers [11, 14, 15, 46, 48, 57]. In line with these findings, the present study found similar patterns for plasma p-tau181 concentrations and PET imaging results with a second-generation tau tracer ( $^{18}\text{F}$ -Florzolotau). Interestingly, these markers also appeared to have an excellent discriminatory ability to distinguish between  $\text{A}\beta+$  and  $\text{A}\beta-$  individuals. Research investigating plasma (p-tau181, p-tau217, and p-tau231) and PET imaging ( $^{18}\text{F}$ -RO948,  $^{18}\text{F}$ -MK-6240, and  $^{18}\text{F}$ -flortaucipir) T biomarkers has generally detected an increasing tau burden from the preclinical stage to clinically overt dementia. Aside from evidence that plasma p-tau levels tend to increase in a less pronounced fashion in symptomatic patients [11, 15, 45, 58–61], the correlations of plasma T biomarkers with the results of neuropsychological testing are generally moderate [17, 45, 48]. The pathophysiological cascade of  $\text{A}\beta-$  and tau-related processes is not constant during disease progression, that is, as opposed to early in the disease, in the advanced stages such as AD dementia when  $\text{A}\beta$  fibrils and soluble p-tau levels have stabilized, cognitive decline is associated with the accumulation rate of insoluble tau aggregates [62]. Our data add to previous evidence by demonstrating that only SUVR values on  $^{18}\text{F}$ -Florzolotau PET imaging – and not plasma T biomarker – increased in a stepwise fashion with the increasing severity of cognitive impairment. This result suggests that plasma and PET imaging T biomarkers may convey information that is at least in part not overlapping, with plasma p-tau181 concentrations being more closely related to  $\text{A}\beta$  pathology and tau PET imaging findings being mainly a reflection of the cognitive impairment severity [46]. However, this possibility requires confirmation given the non-linear increase in plasma p-tau181 concentrations during the course of AD [63]. Another prospective research with different T biomarkers from those of our study consistently indicated that the soluble tau as reflected by elevated plasma p-tau217 and the insoluble tau aggregates as reflected by elevated tau PET ( $^{18}\text{F}$ -RO948 and  $^{18}\text{F}$ -flortaucipir) signals, are optimal predictors for longitudinal tau accumulation in the brains of patients with AD at preclinical and prodromal phases, respectively [18]. Future work in this area should also validate different plasma T biomarkers, which may have differential roles for identifying amyloid pathology [64]. Moreover, since comorbidities such as chronic kidney disease are reported to have a non-negligible impact on the interpretation of plasma p-tau181 and p-tau217 levels [16], further studies exploring their potential impact on tau PET biomarkers are warranted.

Given that neurodegeneration is the final consequence of various pre-existing pathological alterations, research has generally explored the association of N biomarkers with the severity of cognitive impairment and clinical trajectories over time [65]. However,  $^{18}\text{F}$ -FDG PET as an imaging N biomarker also shows diagnostic value among patients present to memory clinics with an uncertain diagnosis [66]. In line with prior studies [14, 67], metaROI SUVR value on  $^{18}\text{F}$ -FDG PET imaging was the only N biomarker capable of distinguishing between  $\text{A}\beta+$  and  $\text{A}\beta-$  individuals, although it underperformed both A and T biomarkers. There is also evidence that, different from other N biomarkers, glucose hypometabolism on  $^{18}\text{F}$ -FDG PET may predict a steeper cognitive decline trajectory; therefore, the traditional classification of  $^{18}\text{F}$ -FDG PET imaging as an N biomarker has been put into question [68]. Interestingly, we found that  $^{18}\text{F}$ -FDG PET outperformed NfL – a plasma N biomarker – in reflecting the severity of cognitive impairment in  $\text{A}\beta+$  individuals. However, the plasma NfL level was superior to  $^{18}\text{F}$ -FDG PET as a marker of disease severity in  $\text{A}\beta-$  individuals – a finding which calls for additional investigations.

While we are not aware of any other study that has provided a head-to-head comparison of plasma and PET imaging ATN biomarkers in relation to the presence of amyloid pathology and the severity of cognitive impairment across the AD spectrum, several design limitations should be acknowledged. Since this single-center investigation was cross-sectional, it is not possible to establish the causal nature or the directionality of the observed associations. We did not obtain longitudinal measures of cognitive impairment, which restricts the prognostic impact of our findings. Meanwhile, the sample size of the final study cohort was limited, and attention needs to be paid to potential sources of bias. We have only enrolled patients presented to a memory clinic and consequently we were unable to include subjects in the preclinical stage. Our findings may be most applicable and generalizable to those with MCI or dementia due to AD. Another limitation is the uneven distribution of amyloid pathology, resulting in more participants within the  $\text{A}\beta+$  group. The uneven distributions of different severities of clinical cognitive impairment, a common drawback of the serial-enrollment design when the study sample size is limited, also requires attention. The present analysis did not include measurements of recently developed plasma T biomarkers (i.e., p-tau217, p-tau231), as well as of neuroinflammatory markers. Because the availability of  $^{18}\text{F}$ -Florzolotau PET imaging is still limited, our results are not conducive to establishing a definitive equivalence between this imaging modality and the combination of plasma p-tau181 and

$^{18}\text{F}$ -FDG PET. Besides, two atlases were used for PET imaging analysis, which may have attenuated some of the results although preceding data rendered such effects likely to be minimal [69]. Last but not least, we took the visual assessment of  $^{18}\text{F}$ -florbetapir PET imaging as a ground truth for  $\text{A}\beta$  status. As semi-quantitative binary cutoffs (i.e., a global SUVR greater than 1.1 indicates positive  $\text{A}\beta$  accumulation) [34, 70] have been recommended for  $^{18}\text{F}$ -florbetapir, it is necessary to further replicate our findings using semi-quantitative measurements as the ground truth.

## Conclusion

The results from the present study raise the possibility that  $^{18}\text{F}$ -florbetapir PET imaging (A),  $^{18}\text{F}$ -Florzolotau PET imaging (T), and plasma p-tau181 (T) can be considered as interchangeable biomarkers in the assessment of  $\text{A}\beta$  status in both MCI and dementia due to AD. The findings on  $^{18}\text{F}$ -Florzolotau PET (T) and  $^{18}\text{F}$ -FDG PET (N) could also serve as imaging markers for the severity of cognitive impairment.

## Abbreviations

AAL3	Automated Anatomical Labelling Atlas three
$\text{A}\beta$	$\beta$ -Amyloid
AD	Alzheimer's disease
APOE	Apolipoprotein E
CDR	Clinical dementia rating
CSF	Cerebrospinal fluid
FAQ	Functional Assessment Questionnaire
FDG	Fluorodeoxyglucose
FWE	Family wise error
GLM	Generalized linear model
MCI	Mild cognitive impairment
metaROI	Meta-analytically derived region of interest
MMSE	Mini-Mental State Examination
MOCA	Montreal Cognitive Assessment
MRI	Magnetic resonance imaging
MTL	Medial temporal lobe
NEO-T	Temporal neocortex
NfL	Neurofilament light chain
PET	Positron emission tomography
p-tau	Phosphorylated tau
SCD	Subjective cognitive decline
SPM12	Statistical Parametric Mapping 12
SUVR	Standardized uptake value ratio

## Supplementary Information

The online version contains supplementary material available at <https://doi.org/10.1186/s40035-023-00365-x>.

**Additional file 1 Fig. S1.** Study flowchart. **Fig. S2.** Reciprocal associations between plasma and PET imaging ATN biomarkers: voxel-wise analysis. **Fig. S3.** Agreement between different PET imaging ATN biomarkers for predicting the  $\text{A}\beta$  status. **Fig. S4.** Plasma and PET imaging ATN biomarkers in relation to the severity of cognitive impairment in  $\text{A}\beta$ - subjects. **Fig. S5.** Plasma and PET imaging ATN biomarkers in relation to the severity of cognitive impairment in the entire cohort. **Fig. S6.** Associations of plasma and PET imaging ATN biomarkers with neuropsychological tests. **Table S1.** Region-level reciprocal associations between plasma and PET imaging

ATN biomarkers. **Table S2.** Plasma and PET imaging ATN biomarkers in relation to the severity of cognitive impairment in  $\text{A}\beta$ + subjects. **Table S3.** Plasma and PET imaging ATN biomarkers in relation to the severity of cognitive impairment in  $\text{A}\beta$ - subjects. **Table S4.** Plasma and PET imaging ATN biomarkers in relation to the severity of cognitive impairment in the entire cohort.

## Acknowledgements

We would like to thank all staff members of the Shanghai Memory Study (SMS) (full list presented in the Consortium list below). We would like to express our sincere appreciation to the study participants and their relatives. We are grateful to APRINOIA Therapeutics for providing the  $^{18}\text{F}$ -Florzolotau precursor.

Keliang Chen<sup>1,2</sup>, Langfeng Shi<sup>1,2</sup>, Wanqing Wu<sup>1,2</sup>, Yan Zhou<sup>1,2</sup>, Yan Zhang<sup>1,2</sup>, Fang Pej<sup>1,2</sup>

<sup>1</sup>National Clinical Research Center for Aging and Medicine & National Center for Neurological Disorders, Huashan Hospital, Fudan University, Shanghai, China, <sup>2</sup>Department of Neurology, Huashan Hospital, Fudan University, Shanghai, China

## Author contributions

Study concept and design: QZ, CZ, YG, JL and XM; acquisition, analysis, or interpretation of data: all authors; drafting of the manuscript: JL and XM; critical revision of the manuscript for important intellectual content: QZ, CZ, YG, TZY, HZ, ZX, ML, ZJ, JW, LC, LZ, JG, XL, WB, PW, and DD.

## Funding

This work was supported by grants from the National Natural Science Foundation of China (81971641, 82071200, 82272039, and 82021002), the ST12030-Major Project (2022ZD0211600), the Clinical Research Plan of Shanghai Hospital Development Center (SHDC2020CR1038B, SHDC2020CR4007), the National Key R&D Program of China (2022YFC2009902, 2022YFC2009900), and Medical Innovation Research Project of Shanghai Science and Technology Commission (21Y11903300).

## Availability of data and materials

Fully anonymized data will be shared upon request from qualified investigators, subject to approval by the China Human Genetic Resources Administration Office. Data transfer will have to comply with the Regulations of the People's Republic of China.

## Declarations

### Ethics approval and consent to participate

This study was approved by the Institutional Review Board of Huashan Hospital. Written informed consent was obtained from all participants or legal guardians.

### Consent for publication

Not applicable.

### Competing interests

Tzu-Chen Yen is an employee of APRINOIA Therapeutics Co., Ltd (Suzhou, China). All other authors have no conflicts of interest to declare.

### Author details

<sup>1</sup>Department of Nuclear Medicine and PET Center, Huashan Hospital, Fudan University, Shanghai, China. <sup>2</sup>National Clinical Research Center for Aging and Medicine and National Center for Neurological Disorders, Huashan Hospital, Fudan University, Shanghai, China. <sup>3</sup>Department of Neurology, Huashan Hospital, Fudan University, Shanghai, China. <sup>4</sup>Department of Ultrasound, Huashan Hospital, Fudan University, Shanghai, China. <sup>5</sup>APRINOIA Therapeutics Co., Ltd, Suzhou, China. <sup>6</sup>Human Phenome Institute, Fudan University, Shanghai, China. <sup>7</sup>MOE Frontiers Center for Brain Science, Fudan University, Shanghai, China.

Received: 19 February 2023 Accepted: 2 June 2023

Published online: 29 June 2023

## References

- Wu YT, Beiser AS, Breteler MMB, Fratiglioni L, Helmer C, Hendrie HC, et al. The changing prevalence and incidence of dementia over time—current evidence. *Nat Rev Neurol*. 2017;13:327–39.
- Jessen F, Amariglio RE, Buckley RF, van der Flier WM, Han Y, Molinuevo JL, et al. The characterisation of subjective cognitive decline. *Lancet Neurol*. 2020;19:271–8.
- Petersen RC. Mild cognitive impairment as a diagnostic entity. *J Intern Med*. 2004;256:183–94.
- Jack CR, Bennett DA, Blennow K, Carrillo MC, Dunn B, Haeberlein SB, et al. NIA-AA research framework: toward a biological definition of Alzheimer's disease. *Alzheimers Dement*. 2018;14:535–62.
- Ossenkoppele R, van der Kant R, Hansson O. Tau biomarkers in Alzheimer's disease: towards implementation in clinical practice and trials. *Lancet Neurol*. 2022;21:726–34.
- Frisoni GB, Boccardi M, Barkhof F, Blennow K, Cappa S, Chiotis K, et al. Strategic roadmap for an early diagnosis of Alzheimer's disease based on biomarkers. *Lancet Neurol*. 2017;16:661–76.
- Dubois B, Villain N, Frisoni GB, Rabinovici GD, Sabbagh M, Cappa S, et al. Clinical diagnosis of Alzheimer's disease: recommendations of the international working group. *Lancet Neurol*. 2021;20:484–96.
- Alawode DOT, Heslegrave AJ, Ashton NJ, Karikari TK, Simrén J, Montoliu-Gaya L, et al. Transitioning from cerebrospinal fluid to blood tests to facilitate diagnosis and disease monitoring in Alzheimer's disease. *J Intern Med*. 2021;290:583–601.
- Mattsson-Carlgrén N, Leuzy A, Janelidze S, Palmqvist S, Stomrud E, Strandberg O, et al. The implications of different approaches to define AT(N) in Alzheimer disease. *Neurology*. 2020;94:E2233–44.
- Mielke MM, Hagen CE, Xu J, Chai X, Vemuri P, Lowe VJ, et al. Plasma phospho-tau181 increases with Alzheimer's disease clinical severity and is associated with tau- and amyloid-positron emission tomography. *Alzheimers Dement*. 2018;14:989–97.
- Janelidze S, Mattsson N, Palmqvist S, Smith R, Beach TG, Serrano GE, et al. Plasma P-tau181 in Alzheimer's disease: relationship to other biomarkers, differential diagnosis, neuropathology and longitudinal progression to Alzheimer's dementia. *Nat Med*. 2020;26:379–86.
- Karikari TK, Pascoal TA, Ashton NJ, Janelidze S, Benedet AL, Rodriguez JL, et al. Blood phosphorylated tau 181 as a biomarker for Alzheimer's disease: a diagnostic performance and prediction modelling study using data from four prospective cohorts. *Lancet Neurol*. 2020;19:422–33.
- Moscato A, Grothe MJ, Ashton NJ, Karikari TK, Rodriguez JL, Snellman A, et al. Time course of phosphorylated-tau181 in blood across the Alzheimer's disease spectrum. *Brain*. 2021;144:325–39.
- Palmqvist S, Janelidze S, Quiroz YT, Zetterberg H, Lopera F, Stomrud E, et al. Discriminative accuracy of plasma phospho-tau217 for Alzheimer disease vs other neurodegenerative disorders. *JAMA*. 2020;324:772.
- Ashton NJ, Pascoal TA, Karikari TK, Benedet AL, Lantero-Rodriguez J, Brinkmalm G, et al. Plasma p-tau231: a new biomarker for incipient Alzheimer's disease pathology. *Acta Neuropathol*. 2021;141:709–24.
- Mielke MM, Dage JL, Frank RD, Algeciras-Schimmich A, Knopman DS, Lowe VJ, et al. Performance of plasma phosphorylated tau 181 and 217 in the community. *Nat Med*. 2022;28:1398–405.
- Coomans EM, Verberk IMW, Ossenkoppele R, Verfaillie SCJ, Visser D, Gouda M, et al. A head-to-head comparison between plasma pTau181 and Tau PET along the Alzheimer's disease continuum. *J Nucl Med*. 2023;64:437–43.
- Leuzy A, Smith R, Cullen NC, Strandberg O, Vogel JW, Binette AP, et al. Biomarker-based prediction of longitudinal tau positron emission tomography in Alzheimer disease. *JAMA Neurol*. 2022;79:149–58.
- Tissot C, Theriault J, Kunach P, Benedet AL, Pascoal TA, Ashton NJ, et al. Comparing tau status determined via plasma pTau181, pTau231 and [<sup>18</sup>F]MK6240 tau-PET. *Ebiomedicine*. 2022;76:103837.
- Yang L, Rieves D, Ganley C. Brain amyloid imaging — FDA approval of florbetapir F18 injection. *N Engl J Med*. 2012;367:885–7.
- Tagai K, Ono M, Kubota M, Kitamura S, Takahata K, Seki C, et al. High-contrast in vivo imaging of Tau pathologies in Alzheimer's and non-Alzheimer's disease tauopathies. *Neuron*. 2021;109:42–58.e8.
- Xiao Z, Wu W, Ma X, Liang X, Lu J, Zheng L, et al. Plasma Aβ42/Aβ40 and p-tau 181 predict long-term clinical progression in a cohort with amnesic mild cognitive impairment. *Clin Chem*. 2022;68:1552–63.
- Guze SB. Diagnostic and Statistical Manual of Mental Disorders, 4th ed. (DSM-IV). *Am J Psychiatry*. 1995;152:1228.
- Jessen F, Amariglio RE, Van Boxtel M, Breteler M, Ceccaldi M, Chételat G, et al. A conceptual framework for research on subjective cognitive decline in preclinical Alzheimer's disease. *Alzheimer's Dement*. 2014;10:844–52.
- McKhann G, Drachman D, Folstein M, Katzman R, Price D, Stadlan E. Clinical diagnosis of Alzheimer's disease: report of the NINCDS-ADRDA work group under the auspices of department of health and human services task force on Alzheimer's disease. *Neurology*. 1984;34:939–44.
- Morris JC. The clinical dementia rating (CDR). *Neurology*. 1993;43:2412.2–2412.a.
- Lim WS, Chong MS, Sahadevan S. Utility of the clinical dementia rating in Asian populations. *Clin Med Res*. 2007;5:61–70.
- Ding D, Zhao Q, Guo Q, Meng H, Wang B, Luo J, et al. Prevalence of mild cognitive impairment in an urban community in China: a cross-sectional analysis of the Shanghai aging study. *Alzheimer's Dement*. 2015;11:300–9.
- Wu X, Xiao Z, Yi J, Ding S, Gu H, Wu W, et al. Development of a plasma biomarker diagnostic model incorporating ultrasensitive digital immunoassay as a screening strategy for Alzheimer disease in a Chinese population. *Clin Chem*. 2021;67:1628–39.
- Shi Z, Fu L, Zhang N, Zhao X, Liu S, Zuo C, et al. Amyloid PET in dementia syndromes: a Chinese multicenter study. *J Nucl Med*. 2020;61:1814–9.
- Liu F-T, Lu J-Y, Li X-Y, Liang X-N, Jiao F-Y, Ge J-J, et al. <sup>18</sup>F-Florbetapir PET imaging captures the distribution patterns and regional vulnerability of tau pathology in progressive supranuclear palsy. *Eur J Nucl Med Mol Imaging*. 2023;50:1395–405.
- Lu J, Wang M, Wu P, Yakushev I, Zhang H, Ziegler S, et al. Adjustment for the age- and gender-related metabolic changes improves the differential diagnosis of parkinsonism. *Phenomics*. 2023;3:50–63.
- Lundeen TF, Seibyl JP, Covington MF, Eshghi N, Kuo PH. Signs and artifacts in amyloid PET. *Radiographics*. 2018;38:2123–33.
- Landau S, Jagust W. ADNI Florbetapir processing methods. 2015. [https://adni.bitbucket.io/reference/docs/UCBERKELEYAV45/ADNI\\_AV45\\_Methods\\_JagustLab\\_06.25.15.pdf](https://adni.bitbucket.io/reference/docs/UCBERKELEYAV45/ADNI_AV45_Methods_JagustLab_06.25.15.pdf)
- Verger A, Doyen M, Campion JY, Guedj E. The pons as reference region for intensity normalization in semi-quantitative analysis of brain 18FDG PET: application to metabolic changes related to ageing in conventional and digital control databases. *EJNMMI Res*. 2021;11:31.
- Rolls ET, Huang CC, Lin CP, Feng J, Joliot M. Automated anatomical labeling atlas 3. *Neuroimage*. 2020;206:116189.
- Desikan RS, Ségonne F, Fischl B, Quinn BT, Dickerson BC, Blacker D, et al. An automated labeling system for subdividing the human cerebral cortex on MRI scans into gyral based regions of interest. *Neuroimage*. 2006;31:968–80.
- Ossenkoppele R, Pichet Binette A, Groot C, Smith R, Strandberg O, Palmqvist S, et al. Amyloid and tau PET-positive cognitively unimpaired individuals are at high risk for future cognitive decline. *Nat Med*. 2022;28:2381–7.
- Knopman DS, Jack CR, Wiste HJ, Lundt ES, Weigand SD, Vemuri P, et al. <sup>18</sup>F-fluorodeoxyglucose positron emission tomography, aging, and apolipoprotein E genotype in cognitively normal persons. *Neurobiol Aging*. 2014;35:2096–106.
- Hansson O, Lehmann S, Otto M, Zetterberg H, Lewczuk P. Advantages and disadvantages of the use of the CSF Amyloid β (Aβ) 42/40 ratio in the diagnosis of Alzheimer's Disease. *Alzheimers Res Ther*. 2019;11:34.
- Leuzy A, Mattsson-Carlgrén N, Palmqvist S, Janelidze S, Dage JL, Hansson O. Blood-based biomarkers for Alzheimer's disease. *EMBO Mol Med*. 2022;14:e14408.
- Janelidze S, Teunissen CE, Zetterberg H, Allué JA, Sarasa L, Eichenlaub U, et al. Head-to-head comparison of 8 plasma amyloid-β 42/40 assays in Alzheimer disease. *JAMA Neurol*. 2021;78:1375–82.
- Morris E, Chalkidou A, Hammers A, Peacock J, Summers J, Keevil S. Diagnostic accuracy of <sup>18</sup>F amyloid PET tracers for the diagnosis of Alzheimer's disease: a systematic review and meta-analysis. *Eur J Nucl Med Mol Imaging*. 2016;43:374–85.
- Jack CR, Knopman DS, Jagust WJ, Petersen RC, Weiner MW, Aisen PS, et al. Tracking pathophysiological processes in Alzheimer's disease: an updated hypothetical model of dynamic biomarkers. *Lancet Neurol*. 2013;12:207–16.

45. Xiao Z, Wu X, Wu W, Yi J, Liang X, Ding S, et al. Plasma biomarker profiles and the correlation with cognitive function across the clinical spectrum of Alzheimer's disease. *Alzheimers Res Ther.* 2021;13:123.
46. Ossenkoppele R, Reimand J, Smith R, Leuzy A, Strandberg O, Palmqvist S, et al. Tau PET correlates with different Alzheimer's disease-related features compared to CSF and plasma p-tau biomarkers. *EMBO Mol Med.* 2021;13:e14398.
47. Janelidze S, Bali D, Ashton NJ, Barthélemy NR, Vanbrabant J, Stoops E, et al. Head-to-head comparison of 10 plasma phospho-tau assays in prodromal Alzheimer's disease. *Brain.* 2022;146(4):1532.
48. Thijssen EH, La Joie R, Strom A, Fonseca C, Iaccarino L, Wolf A, et al. Plasma phosphorylated tau 217 and phosphorylated tau 181 as biomarkers in Alzheimer's disease and frontotemporal lobar degeneration: a retrospective diagnostic performance study. *Lancet Neurol.* 2021;20:739–52.
49. Hsu JL, Lin KJ, Hsiao IT, Huang KL, Liu CH, Wu HC, et al. The imaging features and clinical associations of a novel tau PET tracer - <sup>18</sup>F-APN1607 in Alzheimer disease. *Clin Nucl Med.* 2020;45:747–56.
50. Lu J, Bao W, Li M, Li L, Zhang Z, Alberts I, et al. Associations of [(18)F]-APN-1607 tau PET binding in the brain of Alzheimer's disease patients with cognition and glucose metabolism. *Front Neurosci.* 2020;14:604.
51. Zhang Y, Lu J, Wang M, Zuo C, Jiang J. Influence of gender on tau precipitation in Alzheimer's disease according to ATN research framework. *Phenomics.* 2022. <https://doi.org/10.1007/s43657-022-00076-9>.
52. Li L, Liu FT, Li M, Lu JY, Sun YM, Liang X, et al. Clinical Utility of <sup>18</sup>F-APN-1607 Tau PET Imaging in Patients with progressive supranuclear palsy. *Mov Disord.* 2021;36:2314–23.
53. Zhou X, Lu J, Liu F, Wu P, Zhao J, Ju Z, et al. In vivo <sup>18</sup>F-APN-1607 tau PET imaging in MAPT mutations: cross-sectional and longitudinal findings. *Mov Disord.* 2022;37:525–34.
54. Soleimani-Meigooni DN, Iaccarino L, La JR, Baker S, Bourakova V, Boxer AL, et al. <sup>18</sup>F-flortaucipir PET to autopsy comparisons in Alzheimer's disease and other neurodegenerative diseases. *Brain.* 2020;143:3477–94.
55. Agüero C, Dhaynaut M, Normandin MD, Amaral AC, Guehl NJ, Neelamegam R, et al. Autoradiography validation of novel tau PET tracer [F-18]-MK-6240 on human postmortem brain tissue. *Acta Neuropathol Commun.* 2019;7:37.
56. Malarte ML, Gillberg PG, Kumar A, Bogdanovic N, Lemoine L, Nordberg A. Discriminative binding of tau PET tracers PI2620, MK6240 and RO948 in Alzheimer's disease, corticobasal degeneration and progressive supranuclear palsy brains. *Mol Psychiatry.* 2023;28:1272–83.
57. Milà-Alomà M, Ashton NJ, Shekari M, Salvadó G, Ortiz-Romero P, Montoliu-Gaya L, et al. Plasma p-tau231 and p-tau217 as state markers of amyloid-β pathology in preclinical Alzheimer's disease. *Nat Med.* 2022;28:1797–801.
58. Doré V, Doecke JD, Saad ZS, Triana-Baltzer G, Slemmon R, Krishnadas N, et al. Plasma p217+tau versus NAV4694 amyloid and MK6240 tau PET across the Alzheimer's continuum. *Alzheimers Dement (Amst).* 2022;14:e12307.
59. Leuzy A, Smith R, Ossenkoppele R, Santillo A, Borroni E, Klein G, et al. Diagnostic performance of RO948 F 18 tau positron emission tomography in the differentiation of Alzheimer disease from other neurodegenerative disorders. *JAMA Neurol.* 2020;77:955–65.
60. Mattsson N, Insel PS, Donohue M, Jögi J, Ossenkoppele R, Olsson T, et al. Predicting diagnosis and cognition with <sup>18</sup>F-AV-1451 tau PET and structural MRI in Alzheimer's disease. *Alzheimers Dement.* 2019;15:570–80.
61. Mattsson-Carlgen N, Andersson E, Janelidze S, Ossenkoppele R, Insel P, Strandberg O, et al. Aβ deposition is associated with increases in soluble and phosphorylated tau that precede a positive Tau PET in Alzheimer's disease. *Sci Adv.* 2020;6(16):eaa2387.
62. Pichet Binette A, Franzmeier N, Spotorno N, Ewers M, Brendel M, Biel D, et al. Amyloid-associated increases in soluble tau relate to tau aggregation rates and cognitive decline in early Alzheimer's disease. *Nat Commun.* 2022;13:6635.
63. Suárez-Calvet M, Karikari TK, Ashton NJ, Lantero Rodríguez J, Milà-Alomà M, Gispert JD, et al. Novel tau biomarkers phosphorylated at T181, T217 or T231 rise in the initial stages of the preclinical Alzheimer's continuum when only subtle changes in Aβ pathology are detected. *EMBO Mol Med.* 2020;12:e12921.
64. Ashton NJ, Janelidze S, Mattsson-Carlgen N, Binette AP, Strandberg O, Brum WS, et al. Differential roles of Aβ42/40, p-tau231 and p-tau217 for Alzheimer's trial selection and disease monitoring. *Nat Med.* 2022;28:2555–62.
65. Mattsson N, Cullen NC, Andreasson U, Zetterberg H, Blennow K. Association between longitudinal plasma neurofilament light and neurodegeneration in patients with Alzheimer disease. *JAMA Neurol.* 2019;76:791–9.
66. Perini G, Rodriguez-Veitez E, Kadir A, Sala A, Savitcheva I, Nordberg A. Clinical impact of <sup>18</sup>F-FDG-PET among memory clinic patients with uncertain diagnosis. *Eur J Nucl Med Mol Imaging.* 2021;48:612–22.
67. Brickman AM, Manly JJ, Honig LS, Sanchez D, Reyes-Dumeyer D, Lantigua RA, et al. Plasma p-tau181, p-tau217, and other blood-based Alzheimer's disease biomarkers in a multi-ethnic, community study. *Alzheimers Dement.* 2021;17:1353–64.
68. Ou YN, Xu W, Li JQ, Guo Y, Cui M, Chen KL, et al. FDG-PET as an independent biomarker for Alzheimer's biological diagnosis: a longitudinal study. *Alzheimers Res Ther.* 2019;11:57.
69. Pelkmans W, Ossenkoppele R, Dicks E, Strandberg O, Barkhof F, Tijms BM, et al. Tau-related grey matter network breakdown across the Alzheimer's disease continuum. *Alzheimers Res Ther.* 2021;13:138.
70. Joshi AD, Pontecorvo MJ, Clark CM, Carpenter AP, Jennings DL, Sadowsky CH, et al. Performance characteristics of amyloid PET with florbetapir F 18 in patients with Alzheimer's disease and cognitively normal subjects. *J Nucl Med.* 2012;53:378–84.

Ready to submit your research? Choose BMC and benefit from:

- fast, convenient online submission
- thorough peer review by experienced researchers in your field
- rapid publication on acceptance
- support for research data, including large and complex data types
- gold Open Access which fosters wider collaboration and increased citations
- maximum visibility for your research: over 100M website views per year

At BMC, research is always in progress.

Learn more [biomedcentral.com/submissions](https://biomedcentral.com/submissions)

